CORTICAL SHELL THICKNESS AND ITS CONTRIBUTION TO VERTEBRAL BODY STIFFNESS

Harun H Bayraktar (1,3), Jenni M Buckley (1,3), Mark F Adams (2)
Atul Gupta (1), Paul F Hoffmann (1,3), David C Lee (1,4)
Panayiotis Papadopoulos (3), Tony M Keaveny (1,3,4)

(1) Orthopaedic Biomechanics Laboratory
University of California, Berkeley, CA

(2) Computational Sciences, Computer Sciences and Mathematics Center, Sandia National Laboratories, Livermore, CA

(3) Department of Mechanical Engineering
University of California, Berkeley, CA

(4) Department of Bioengineering
University of California, Berkeley, CA

INTRODUCTION

Fracture risk prediction is key in diagnosis of vertebral osteoporosis. However, the structural role of the cortical shell remains controversial. While some studies have concluded that the shell takes over 45% of the load [1, 2], others have concluded it takes less than 15% [3, 4]. Furthermore, different thickness measures of the cortical shell have been reported [5, 6]. With advances in micro-CT imaging technology and high-performance supercomputing, it is now possible to measure cortical shell thickness in a comprehensive fashion, and analyze tissue level stress distributions using high-resolution finite element modeling (μFE) at the whole bone scale. While this method has been applied to the human proximal femur [7], no such studies exist for the human vertebra.

The overall goal of this study was to investigate the role of cortical shell in vertebral body mechanical behavior. Specifically, our objectives were to: 1) digitally identify, remove, and measure the volume and thickness of the cortical shell, using μCT scans at 40 μm resolution, 2) use a μFE model of the entire vertebral body to obtain apparent stiffness and tissue strain histograms with and without the shell and also the shell alone, 3) calibrate a generic finite element model to match the contribution of the shell in the μFE model and from that determine an effective elastic modulus of the shell for use in continuum level models.

METHODS

One human T-10 vertebral body from an 82 year old female was used in this study. After removal of the posterior elements, the vertebral body was scanned at 30 μm resolution using μCT (Scanco 80, Bassersdorf, Switzerland). Using regional averaging, the resolution was decreased to 40 μm to save computational time. Custom software was developed to automatically identify and remove the voxels associated with the cortical shell (Fig. 1). Average shell thickness and total shell volume were also calculated.

Three μFE models of the vertebral body were created by converting voxels directly into finite elements: 1) with shell, 2) without shell, and 3) shell-only. Due to the very large size of the models (Table 1), only half of the vertebral body was analyzed using mid-saggital plane with symmetry boundary conditions. A 1% compressive strain was applied in the superior-inferior direction. Models were run on a IBM SP3 parallel supercomputer using 1024 processors and 512 GB of memory. A custom code with a parallel mesh partitioner and multigrid solver [8] was used for linear analysis using a tissue-level Young's modulus of 1 GPa and Poisson's ratio of 0.3. Stiffness was calculated for each model as well as maximum principal strains for each element.

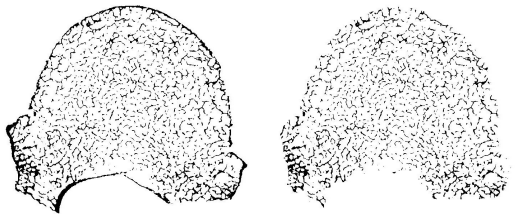

Figure 1. A layer of the μCT scan of the vertebral body (left). Same layer after the voxels identified as part of the cortical shell are removed.

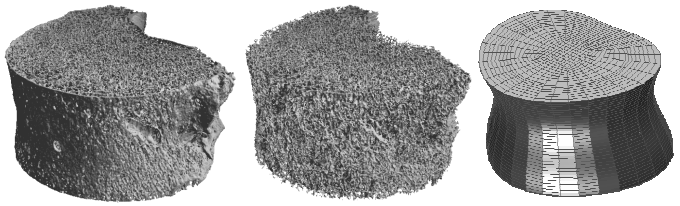

Figure 2. Vertebral body μFE model with (left) and without (center) the cortical shell. Geometry based generic model with shell (right).

A generic finite element model of a representative vertebral body with 2448 quadratic elements was generated (Fig. 2) based on morphology data [9]. The trabecular centrum was modeled as a homogeneous, transversely isotropic continuum, while the cortical shell was modeled using shell elements of 0.3 mm thickness, based on the average value obtained from the μCT image. Six cubic (6 mm side length) μFE models extracted from the trabecular centrum were used

to determine the mean anisotropy ratio (E_{axial}/E_{trans}=4.2) [10]. Using the volume fractions of the six cubes in an experimental modulus-density regression [11] the mean axial modulus for the trabecular centrum (338 MPa) was determined. Remaining elastic constants were calculated using the anisotropy ratio and the axial modulus. The change in apparent level stiffness ($\Delta K/K_S$) with and without the cortical shell was then determined for cortical shell modulus values ranging from 1 to 20 GPa, and the modulus that produced agreement with the μFE model was identified. Linear analyses of the generic model required on average 2 minutes CPU time (Abaqus v6.2, HKS, Pawtucket, RI) on an engineering workstation.

RESULTS

The cortical shell constituted 22.4% of the total bone tissue volume and had an average thickness of 0.31 mm, in close agreement with previously reported measurements [6]. The apparent level stiffness reduction upon removal of the cortical shell was 44% (Table 1). Bimodular strain histograms were indicative of tissue level bending in all three models (Fig. 3).

Calibration of the generic model to match the 44% reduction in apparent level stiffness seen in the μFE model resulted in an effective cortical shell modulus of 14.7 GPa. Using this value, the stiffness of the isolated shell was 12% of the intact vertebral body, just slightly higher than the μFE result (9%).

Table 1. Vertebral body μFE model results

Model	# of elements	CPU time[a] (hrs)	Mean ± SD Strain[b] (%)	Stiffness (N/mm)
With Shell	23,644,335	923	-0.42 ± 0.57	3141
No Shell	18,594,683	454	-0.30 ± 0.53	1762
Shell Only	4,979,992	27	-0.11 ± 0.41	254

[a] Wall clock time for the largest model was 54 minutes on 1024 processors.
[b] Calculated from maximum principal strains in each finite element

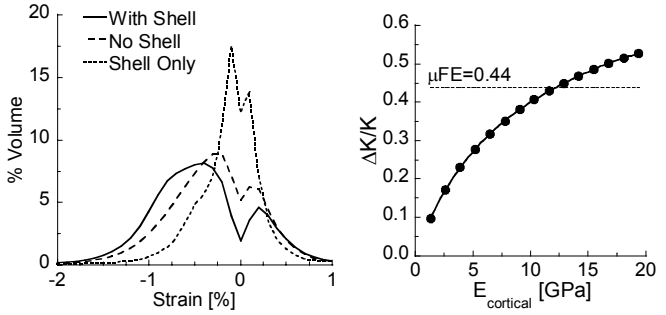

Figure 3. Histograms of maximum principal strains in the tissue for the three μFE models (left). Stiffness reduction vs. effective cortical shell modulus (right). The μFE value is shown with a dashed line.

DISCUSSION

Our results indicate that the cortical shell plays an important role in vertebral body mechanical behavior. Although the isolated cortical shell has an axial stiffness that is only 8% of that of the intact vertebral body, and occupies 22.4% of the total bone volume, removal of the shell resulted in a 44% reduction in stiffness (Table 1). These findings imply the shell and trabecular centrum display a mechanical interaction that cannot be explained by simple load sharing. From the strain histograms (Fig. 3) it is evident that the removal of the shell results in an increase in the volume of tissue at zero-strain. This suggests that the role of the cortical shell is to maximize the load carrying capacity of the trabecular bone by providing load transfer paths to the edge trabeculae that otherwise would be unloaded.

The cortical shell effective modulus of 14.7 GPa for the generic model was lower but comparable to the tissue modulus of 22.5 GPa measured for vertebral cortical tissue using nanoindentation [12]. The difference between these values can be attributed to the effects of shell porosity and geometry, both of which were homogenized in the generic model. However, these effects were indirectly incorporated in the generic model through the calibration with the μFE model behavior.

In conclusion, our results indicate that the cortical shell plays a potentially important structural role by transferring load to the centrum. Furthermore, the calibrated generic finite element model accurately captures this mechanical interaction. We believe these models can be used to parametrically study the effects of variations in the material properties of the centrum and shell that may arise due to osteoporosis.

ACKNOWLEDGEMENTS

NIH AR43784, NPACI-UCB266, NDRI, DOE Grants DE-FG03-94ER25219, DE-FG03-94ER25206. We would also like to thank Michael Liebschner for imaging, Kerem Bülbül and Benjamin Wong for technical assistance.

REFERENCES

1. Rockoff, S.D., et al., 1969, "The relative contribution of trabecular and cortical bone to the strength of human lumbar vertebrae," Calcified Tissue Research, Vol. 3, pp. 163-175.
2. Homminga, J., et al., 2001, "Osteoporosis changes the amount of vertebral trabecular bone at risk of fracture but not the vertebral load distribution," Spine, Vol. 26, pp. 1555-61.
3. McBroom, R.J., et al., 1985, "Prediction of vertebral body compressive fracture using quantitative computed tomography," Journal of Bone and Joint Surgery, Vol. 67-A, pp. 1206-1214.
4. Silva, M.J., et al., 1997, "Load sharing between the shell and centrum in the lumbar vertebral body," Spine, Vol. 22, pp. 140-150.
5. Ritzel, H., et al., 1997, "The thickness of human vertebral cortical bone and its changes in aging and osteoporosis: a histomorphometric analysis of the complete spinal column from thirty-seven autopsy specimens," Journal of Bone and Mineral Research, Vol. 12, pp. 89-95.
6. Silva, M.J., et al., 1994, "Direct and computed tomography thickness measurements of the human lumbar vertebral shell and endplate.," Bone, Vol. 15, pp. 409-414.
7. Van Rietbergen, B., et al., 2000, "Trabecular bone tissue strains in the healthy and osteoporotic human femur."Trans. Orthop. Res. Soc., Orlando, Vol. 25, pp. 33.
8. Adams, M.F., 2000, "Parallel multigrid solvers for 3D unstructured finite element problems in large deformation elasticity and plasticity," International Journal for Numerical Methods in Engineering, Vol. 48, pp. 1241-1262.
9. Berry, J.L., et al., 1987, "A morphometric study of human lumbar and selected thoracic vertebrae," Spine, Vol. 12, pp. 362-367.
10. Van Rietbergen, B., et al., 1996, "Direct mechanics assessment of elastic symmetries and properties of trabecular bone architecture," Journal of Biomechanics, Vol. 29, pp. 1653-1657.
11. Kopperdahl, D.L., et al., 2002, "Quantitative computed tomography estimates of the mechanical properties of human vertebral trabecular bone," J Orthop Res, Vol. 20, pp. 801-5.
12. Rho, J.Y., et al., 1997, "Elastic properties of human cortical and trabecular lamellar bone measured by nanoindentation," Biomaterials, Vol. 18, pp. 1325-30.